coatings

MDPI

Article

Enhancing Flame-Retardant Properties of Polyurethane Composites Using N-β-(Aminoethyl)-γ-aminopropyl Trimethoxysilane and Carbon Black Co-Modified Ammonium Polyphosphate

Lisha Fu [1], Wanjun Hao [1,*], Baoluo Xu [1], Kexi Zhang [1], Jianhua Bi [1], Jingxing Wu [1] and Zhong Wang [2]

[1] State Key Laboratory of South China Sea Marine Resources Utilization, School of Materials Science and Engineering, Hainan University, Haikou 570228, China; fls_0209@163.com (L.F.); 21220856000064@hainanu.edu.cn (B.X.); zhangkexi@hainanu.edu.cn (K.Z.); 20085600210001@hainanu.edu.cn (J.B.); 20080500210032@hainanu.edu.cn (J.W.)

[2] Hainan Sequoia Technology Co., Ltd., Haikou 570208, China; 21220856000016@hainanu.edu.cn

* Correspondence: hwj8899@hainanu.edu.cn; Tel.: +86-157-9903-1033

Abstract: The search for a straightforward method to obtain efficient, affordable, and long-lasting flame retardants with both desirable flame-retardant and mechanical properties for polyurethane (PU) composites remains a significant challenge. In this study, the surface of ammonium polyphosphate (APP) was modified using N-β-(aminoethyl)-γ-aminopropyl trimethoxysilane (KH792) via an ion-exchange reaction, and the modified APP was coated with nanoscale carbon black (CB) to obtain CBAPP. CBAPP demonstrated good compatibility within the PU matrix and notably increased the tensile strength of the PU composites. Furthermore, CBAPP significantly enhanced the flame-retardant properties of the PU composites. The CBAPP/PU composite with a CBAPP mass fraction of 20% achieved a limiting oxygen index of 41.5% and a UL-94 class of V-0. According to the results of this study, our modification approach can be applied to develop other high-performance flame-retardant polymer-based composites, representing a significant contribution to the field of fire safety materials.

Keywords: N-β-(aminoethyl)-γ-aminopropyl trimethoxysilane (KH792); carbon black (CB); flame retardant; polyurethane (PU); ammonium polyphosphate (APP)

check for updates

Citation: Fu, L.; Hao, W.; Xu, B.; Zhang, K.; Bi, J.; Wu, J.; Wang, Z. Enhancing Flame-Retardant Properties of Polyurethane Composites Using N-β-(Aminoethyl)-γ-aminopropyl Trimethoxysilane and Carbon Black Co-Modified Ammonium Polyphosphate. *Coatings* **2024**, *14*, 1126. https://doi.org/10.3390/coatings14091126

Academic Editor: Arūnas Ramanavičius

Received: 13 June 2024
Revised: 23 August 2024
Accepted: 26 August 2024
Published: 2 September 2024

Copyright: © 2024 by the authors. Licensee MDPI, Basel, Switzerland. This article is an open access article distributed under the terms and conditions of the Creative Commons Attribution (CC BY) license (https://creativecommons.org/licenses/by/4.0/).

1. Introduction

Polyurethane (PU) [1,2] sealants are characterized by good film-forming ability and mechanical properties, chemical resistance, abrasion resistance, and wide substrate suitability, and they are mainly used as protective coatings for construction materials, textiles, wood, leather, and metals [3–6]. However, the chemical composition and structure of PU endow it with a high flame propagation rate and high susceptibility to ignition [7]. Moreover, when heated, PU releases a large amount of toxic gases [8,9], which are damaging to human health and the environment, significantly reducing escape time. Therefore, it is imperative to enhance the flame-retardant properties of PU to mitigate its inherent fire risk [9,10]. Adding flame retardants to sealing materials is a common means to make them flame-retardant. Common flame retardants include the halogen flame retardant, inorganic hydroxide flame retardant, and expansion flame retardant. Expansion flame retardant has attracted much attention because of its characteristics of green environmental protection and efficient flame retardance. This retardant has been rapidly developed in recent years. It is composed of acid sources, gas sources, and carbon sources. In the process of combustion, the dehydration and esterification of the acid source and carbon source promote the formation of a carbon layer, and the gas source can make the carbon layer expand. This expanded and dense carbon layer will play a role in oxygen isolation, the insulation of heat, and the

prevention of droplets. When the expansion flame retardant is applied to polyurethane, because polyurethane is generally composed of C, H, and O, which can be used as a carbon source, polyurethane can react with the acid source to promote the formation of a dense carbon layer [11–13]. Therefore, polyurethane sealant is matched in terms of acid sources and gas sources and can form an expansion-type flame-retardant material.

Phosphoric acid and ammonia gas formed by ammonium polyphosphate (APP) at high temperature can be used as acid sources and gas sources, respectively, and can be used as suitable flame retardants for polyurethane sealant in theory. Ammonium polyphosphate (APP) [14,15] is an inorganic flame retardant with high phosphorus and nitrogen content, excellent thermal stability, low smoke emission, and nontoxic properties, aligning with the principles of green development. Owing to these properties, APP has become a research focus in the field of flame-retardant additives [16]. APP has been reported to have a relatively low degree of polymerization, is easily soluble in water, and has poor compatibility with organic material substrates, severely limiting the use of flame-retardant plastics in humid environments [17,18]. Compared with other flame retardants, APP has been widely used in PU flame-retardant composites owing to its high phosphorus content (31 wt%) and ability to form a high-quality carbon layer in PU composites [19]. Synergists are used to reduce the amount of flame retardant added. They are mainly applied in the form of nanofillers (e.g., carbon black [CB], carbon nanotubes [CNTs], OMMT, GO, and metal oxides), which cannot be uniformly distributed in polymer matrixes through simple material processing [20,21]. Microencapsulation or surface modification [22] are effective methods to improve the interfacial bonding and mechanical properties of polymeric materials. Microencapsulation technology [23,24] enhances the interfacial bonding, mechanical properties, flame retardancy, and smoke suppression ability of materials. CB nanoparticles [25,26], one of the most widely used carbon nanomaterials, have garnered considerable attention owing to their abundant sources, low cost, excellent thermal stability, and permanent electrical conductivity. In a previous study, CB was introduced as a nanoscale flame retardant into pure PP, PP/CNT, and PP/carbon fiber systems to improve thermal stability and flame retardancy [27]. CB played an important role in the entrapment of free radicals and the formation of networks within the PP composites [25].

In this study, the surface of APP was modified with KH792 through an ion-exchange reaction [28], and then the modified APP was coated with nano-CB to prepare CBAPP. N-β-(aminoethyl)-γ-aminopropyl trimethoxysilane (KH792) is introduced in this study. The compound possesses inherent crosslinking properties [16] and acts as a CB binder, while silicone polymers have a certain flame-retardant effect [29]. The structures of APP and CBAPP were characterized through Raman spectroscopy, scanning electron microscopy (SEM), and X-ray photoelectron spectroscopy (XPS). CBAPP was added to PU to prepare PU flame-retardant composites, and the mechanical properties of the composites were tested. The thermal stability and flame retardancy of the PU flame-retardant composites were investigated through thermogravimetry (TG) analysis and limiting oxygen index (LOI) and vertical combustion (UL-94) experiments. Afterward, the flame-retardation mechanism of the PU flame-retardant composites was analyzed.

2. Materials and Methods

2.1. Materials

KH792 (industrial-grade, Jinan Xingfeilong Chemical Co. Ltd., Jinan, China); APP (industrial-grade, polymerization degree $n \geq 1000$, Beijing Dehang Wuzhou Science and Technology Co., Ltd., Beijing, China); nanoscale CB (purity > 99%, initial particle size of 30 nm, Shanghai Cabot Chemical Co., Ltd., Shanghai, China); ethanol (95%, analytically pure, Sinopharm Group Chemical Reagent Co., Ltd., Shanghai, China); deionized water (laboratory-made); waterborne PU (industrial-grade, Nippon Coatings Co., Shanghai, China).

2.2. Preparation of Ammonium Polyphosphate Coated with Carbon Black (CBAPP)

CBAPP composites with varying CB contents were prepared by linking CB nanoparticles with APP via KH792. First, a 500 mL round-bottom flask was fitted with a mechanical stirrer, thermometer, and reflux condenser under a nitrogen atmosphere. Subsequently, 70 g of APP and 5 g of KH792 were added to 200 mL of anhydrous ethanol in the flask, and the mixture was stirred for 1 h at room temperature. The mixture was then heated to reflux temperature, and the reaction was maintained until no ammonia was released. The nano-CB was then dispersed in a solution comprising 100 mL of ethanol and 100 mL of deionized water through sonication for 30 min. The modified APP mixture was added to the nano-sized CB solution at 50 °C, and the mixture was stirred under sonication for 30 min to obtain CBAPP. Subsequently, the temperature was increased to 80 °C and maintained for 4 h. Finally, the mixture was filtered to remove the solvent (yielding a colorless clear liquid filtrate). The crude product was washed three times with deionized water and then vacuum-dried at 80 °C for 8 h to eliminate residual solvent. For clarity, 100 wt% APP particles coated with 3 wt%, 6 wt%, 9 wt%, and 12 wt% of nano-CB were designated as 3% CBAPP, 6% CBAPP, 9% CBAPP, and 12% CBAPP, respectively. A schematic of the CBAPP synthesis is shown in Figure 1.

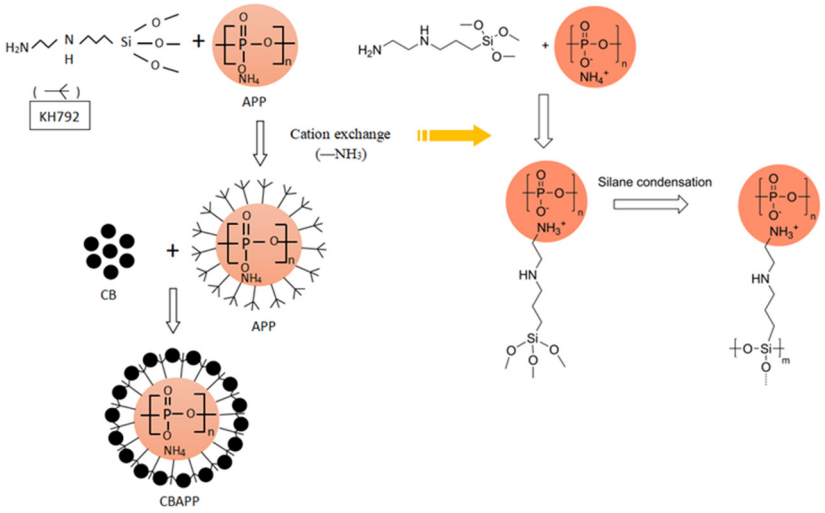


Figure 1. Synthesis route and structure of CBAPP.

2.3. Preparation of Polyurethane Composites

APP and CBAPP were added to PU at a mass fraction of 20%, respectively, to form separate mixtures, which were thoroughly mixed with a high-speed mixer to produce PU flame-retardant composites. The formulations are given in Table 1.

Table 1. Formulation of polyurethane composites.

Sample	PU	APP	3% CBAPP	6% CBAPP	9% CBAPP	12% CBAPP
PU	100					
PU1	80	20				
PU2	80		20			
PU3	80			20		
PU4	80				20	
PU5	80					20

2.4. Testing and Characterization

A Raman test was conducted using an inVia model Raman spectrometer (Renishaw, UK) under argon ion laser excitation at 514 nm with backscattering geometry. An X-ray

diffraction test (XRD) was conducted using a Smart Lab X-ray diffractometer (Rigaku, Japan) with Cu targets, a regulated scanning rate of 3 °/s, and a scanning range of 5–60°. XPS measurements were conducted under ultrahigh-vacuum conditions with AlKα excitation radiation (hν = 1486.6 eV). The micro-morphologies of the fracture surfaces of the APP, CBAPP, and PU composites were examined via SEM (S-3000N, Hitachi, Japan), and the samples were gold-plated before testing. Thermal stability was analyzed using a TL9000 thermogravimetric–infrared imaging–gas chromatography in situ reaction system (PerkinElmer Co., Ltd.) in a N_2 atmosphere, with a temperature increase rate of 20 °C/min over the range of 30–800 °C. The temperature of the samples was measured using a thermogravimetric–infrared imaging–gas chromatography in situ reaction system (TL9000) with a N_2 atmosphere. The LOI was measured using a JF-3A oxygen index tester (Jiangsu Zhuoheng Measurement and Control Technology Co., Ltd., China) according to test standard GB/T2406, with the sample dimensions set at 80 × 10 × 4 mm. According to the UL-94 test standard, vertical combustion was measured using an SH5300 vertical combustion tester (Guangzhou Xinhe Electronic Equipment Co., Ltd., Guangzhou, China) following the guidelines of vertical combustion level GB/T2408, with the sample dimensions set at 130 × 12.8 × 12.8 mm. According to the GB/T 5210-2006 standard, the mechanical properties of the materials were tested using the universal testing machine AI-7000-SU2 at a speed of 50 mm/min. Contact-angle experiments were conducted on a JY-82C contact-angle meter with a droplet volume of 16 μL.

3. Results

3.1. Characterization of CBAPP Structure and Properties

3.1.1. Raman Analysis

The Raman spectra of APP and CBAPP are shown in Figure 2a. The Raman spectrum of APP did not show any peaks at 1300–1600 cm^{-1}. As a typical carbon material, CB showed two strong Raman peaks at approximately 1595 cm^{-1} and 1350 cm^{-1}, designated as the G band (graphite phase, ordered carbon) and the D band (amorphous carbon), respectively. After the nano-CB was deposited on the APP surface, the Raman spectrum of CBAPP featured absorption peaks at the G and D bands, and the intensity of the G and D bands increased with nano-CB addition. According to the Raman spectra, the nano-CB was successfully encapsulated on the APP.

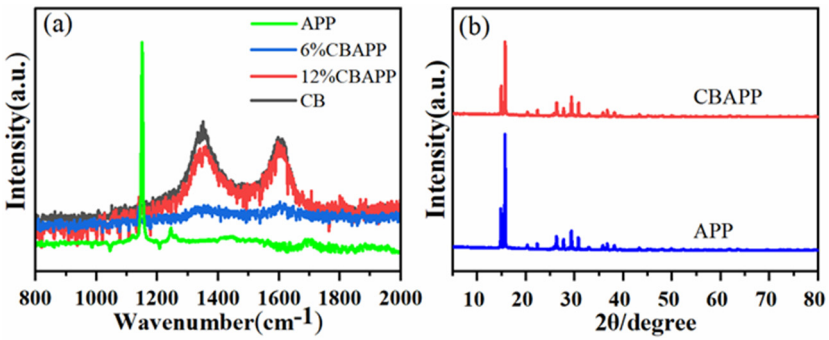


Figure 2. Raman (**a**) and XRD (**b**) spectra of APP and CBAPP.

The effects of KH792 and CB modification on the crystal structure of APP were investigated via XRD Figure 2b. The curves of APP and CBAPP agreed well, and the positions of the characteristic peaks were basically the same. After modification, the positions of the diffraction characteristic peaks of APP did not change. In addition, the XRD spectra of CBAPP featured no new peaks, indicating that the APP crystal structure was not destroyed after modification. The FTIR spectra of PU, APP/PU, and CBAPP/PU are shown in Supplementary Figure S1. The addition absorption peaks of APP and CBAPP did not change because carbon black was coated on the surface of ammonium polyphosphate.

3.1.2. XPS Analysis

To further confirm the chemical compositions of the produced CBAPP surfaces, APP and CBAPP were analyzed via XPS. With the increase in CB content, the N, O, and P contents of CBAPP decreased, while the C content significantly increased. As shown in Figure 3a, the P_{2p} peak located near 134 eV, the P_{2s} peak near 191 eV, and the N_{1s} near 400 eV decreased significantly after modification, while the C_{1s} peak near 285 eV became significantly stronger, which indicates that CB was encapsulated on the APP surface. Moreover, the Si_{2p} peak appeared near 103 eV for the modified CBAPP (Figure 3b), indicating that KH792 was successfully grafted on the APP surface. Figure 3c,d display the N_{1s} fits of APP and CBAPP, respectively. The peak near 399.8 eV in the N_{1s} profile of APP corresponds to NH_4^+, while the NH_4^+ peak still exists in the N_{1s} profile of CBAPP, indicating that only part of NH_4^+ was replaced by NH_3^+ [30]. In addition, a new peak appeared at 402.6 eV, which indicates the occurrence of an ion-exchange reaction between $-NH_2$ in KH792 and NH_4^+ in APP to form a C–NH_3^+ bond.

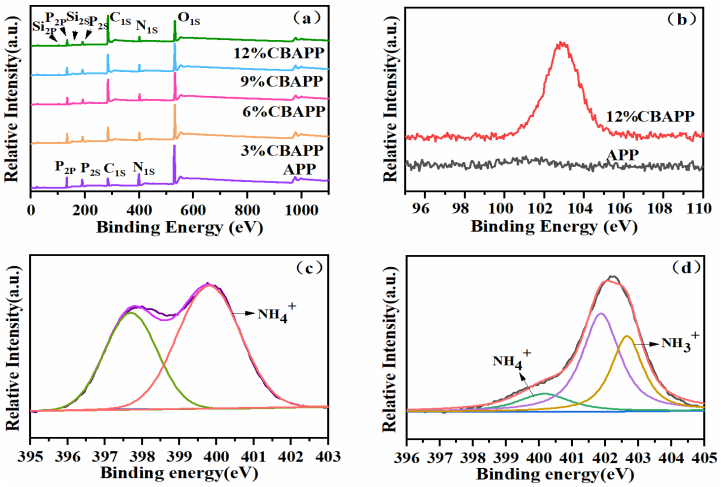


Figure 3. XPS spectra: (**a**) APP and CBAPP; (**b**) APP and CBAPP of Si_{2p}; (**c**) N_{1s} of APP; (**d**) N_{1s} of CBAPP.

3.1.3. SEM

The particle size and surface morphology of particles can be visually, accurately, and effectively characterized via SEM. The SEM images of APP and CBAPP are shown in Figure 4. The unmodified APP powder exhibited a smooth and neat surface, while the CBAPP surface exhibited abundant aggregated small particles, resulting in a rough surface at the micro-nanoscale. This indicates that the CB nanoparticles were successfully immobilized on the APP surface through the attachment of KH792.

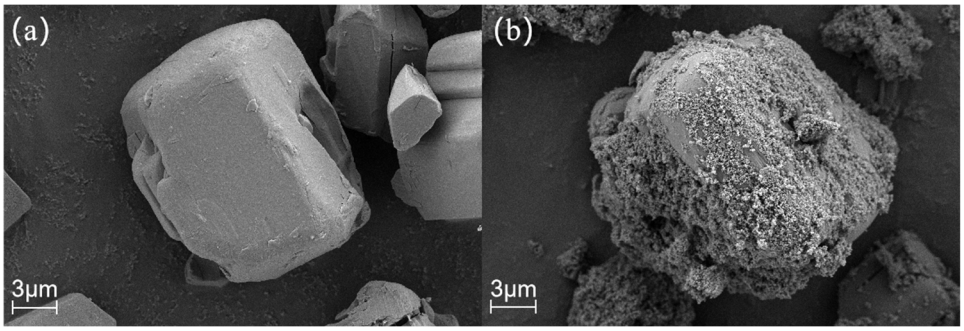


Figure 4. SEM images of APP (**a**) and CBAPP (**b**).

3.1.4. Thermal Stability of APP and CBAPP

The TGA and DTG curves of APP and CBAPP are shown in Figure 5 and Table 2. The initial degradation temperature ($T_{-5\%}$) of APP was 334.1 °C. The thermal decomposition of APP can be roughly divided into two phases: the first phase occurred around 300–500 °C, during which NH_4^+ decomposed to generate ammonia, which overflowed out of the system [31]. Additionally, polyphosphoric acid in the condensed phase underwent dehydration to generate pyrophosphoric acid, with a small amount of water being released. The second stage occurred at approximately 500–650 °C. During this stage, the pyrophosphoric acid generated in the previous stage further decomposed into phosphoric acid, phosphoric acid fragments, and phosphorus oxides, accompanied by a small amount of NH_3 precipitation. The mass loss in the second stage was more significant, and the temperatures corresponding to the maximum weight loss rates in the first and second stages were 342.9 °C and 611.3 °C, respectively. In the CBAPP curves, the temperatures corresponding to the first two maximum heat weight loss rates were 332.7 °C and 619.1 °C [21], respectively. Compared with APP, which stabilized at 800 °C, with a residual amount of 15.4%, CBAPP exhibited a significantly higher residual amount (38.3%) at the same temperature. This indicates that the Si–O–Si network structure on the APP surface and the CB slowed down the decomposition of APP, thereby enhancing its thermal stability before 800 °C. Moreover, a significant thermal weight loss peak appeared at 600–650 °C (Figure 5b). This is attributable to the pyrolysis of CB, leading to the loss of protection and subsequent further decomposition of APP at high temperatures.

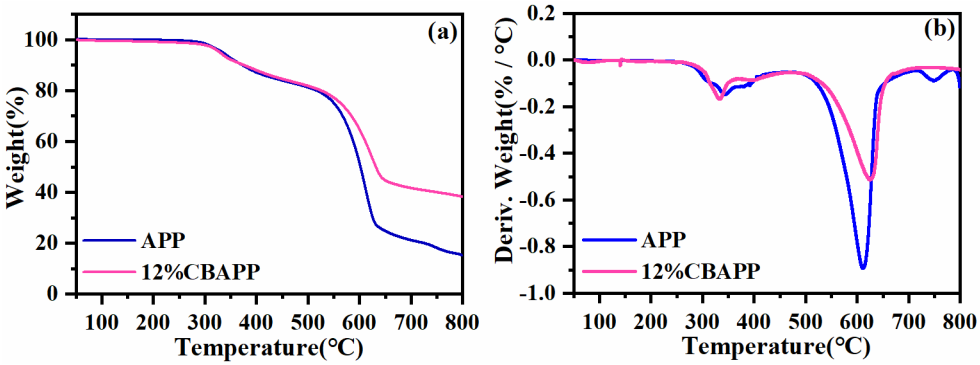


Figure 5. TGA (**a**) and DTG (**b**) curves of APP and CBAPP.

Table 2. TGA and DTG data for PU, APP/PU, and CBAPP/PU.

Samples	$T_{-5\%}$/°C	T_{max1}/°C	T_{max2}/°C	Residual Amount at 800 °C/wt%
PU	390.9	423.6	459.1	44.2
APP/PU	344.3	353.0	432.1	58.1
12% CBAPP/PU	350.4	355.2	429.9	60.7

3.1.5. Contact-Angle Measurements

Wettability is determined by both the chemical composition and microscopic morphology of a material's surface. Macroscopic differences in material surfaces can be identified through contact-angle measurements. The contact angles of the APP and CBAPP particles were measured, and the results are shown in Figure 6. The presence of hydroxyl and ammonium ions on the APP surface resulted in a contact angle of 19.9°, indicating strong polarity and high surface energy. After modification by KH792 and CB, the NH_4^+ on the APP surface was reduced and replaced by a large amount of CB, and the contact angle of CBAPP was 77.9°, indicating good hydrophobicity. The CBAPP surface exhibited enhanced compatibility with organic polymers and reduced hygroscopicity compared with APP.

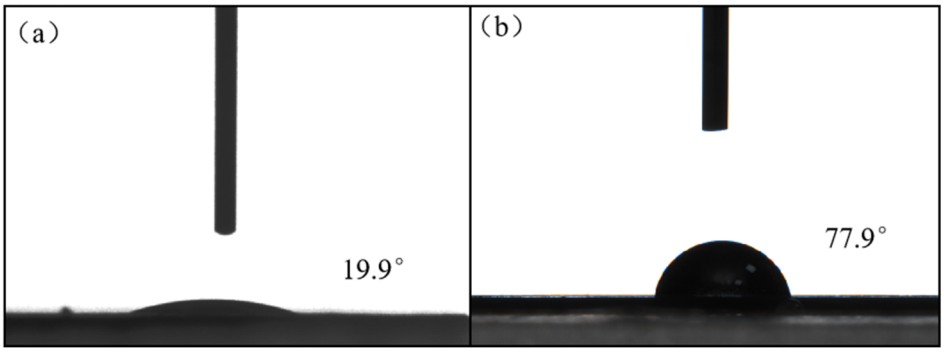


Figure 6. Photograph of the static contact angle of a water droplet on APP (**a**) and CBAPP (**b**).

3.2. Performance Analysis of CBAPP/PU Composites

3.2.1. Mechanical Properties and Water Resistance Test

To elucidate the effects of APP and CBAPP on the mechanical properties of PU composites, we conducted tensile test experiments Figure 7a. The effective dispersion of the additives in the polymer matrix significantly enhanced the mechanical properties of the composites. The presence of APP significantly reduced the tensile strength of the PU composites. Some isocyanate groups (–NCO) in the PU reacted with the amino group in KH792 to form covalent bonds, which facilitated the dispersion of CBAPP particles in the PU. The chemical reaction is illustrated in Figure 8. The tensile strength of APP/PU (0.53 MPa) was ~29% lower than that of pure PU (0.75 MPa); the compatibility between ammonium polyphosphate and polyurethane is poor. However, the tensile strength of the PU composites increased with the CBAPP content. The greater the amount of CB on the APP surface, the higher the tensile strength of the PU composites. The PU composite containing 12% CBAPP exhibited the highest tensile strength at 1.94 MPa, approximately 72% higher than that of the APP/PU composite.

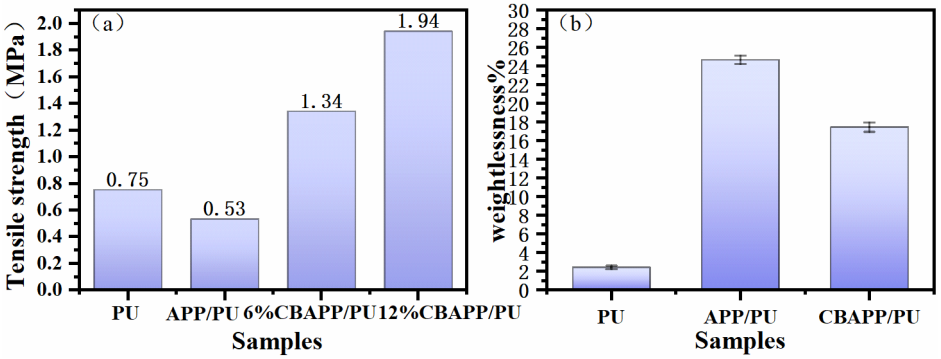


Figure 7. Effects of APP and CBAPP addition on (**a**) tensile properties and (**b**) water resistance.

As depicted in Figure 7b, pure PU exhibited a weight loss of 2.4% after soaking in pure water for 7 days and subsequently drying at room temperature for 3 days. This loss was primarily due to the precipitation of inorganic fillers within the PU. APP/PU exhibited a weight loss of 24.7%. A comparison of APP/PU with pure PU indicated that most of the added APP precipitated, attributable to the abundance of hydrophilic groups on the APP surface, leading to poor compatibility with the organic polymer PU. During the soaking process, water penetration further facilitated the withdrawal of APP from the interior of the PU, resulting in a significant decrease in the APP content of APP/PU. CBAPP/PU exhibited a weight loss of 24.2%, which was marginally lower than that of APP/PU. The non-significant difference in weight loss between both materials was due to the low CB content in CBAPP/PU. CB encapsulated the hydrophilic groups on the APP surface, which might result in a localized interpenetrating network structure at the interface, thereby reducing the precipitation of CBAPP during the soaking process.

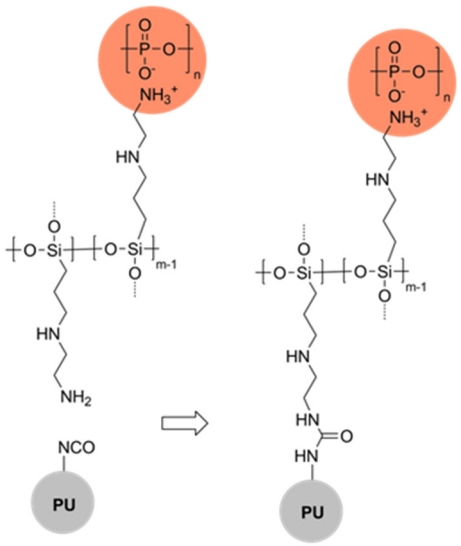


Figure 8. Chemical reaction of isocyanate with amino group.

3.2.2. Thermal Stability of PU, APP/PU, and CBAPP/PU

The TGA and DTG curves of the PU and CBAPP/PU composites are displayed in Figure 9, and the corresponding data are presented in Table 3. The initial decomposition temperature ($T_{-5\%}$) of pure PU was 390.9 °C. The maximum thermal weight loss rate peak appeared at 423.6 °C, and 44.2 wt% of residual carbon remained at 800 °C. The reason for the relatively high residual amount is that the formula of PU contains inorganic components such as $CaCO_3$ and SiO_2. The thermal decomposition of pure PU was mainly due to the thermal decomposition of the main chain, which involved the further degradation of polyol and isocyanate. The two composites APP/PU and CBAPP/PU exhibited lower onset decomposition temperatures and higher residual carbon rates than PU. The flame-retardant PU composites exhibited a lower initial decomposition temperature owing to the lower decomposition temperature of the added flame-retardant APP. Additionally, the polyphosphoric acid generated from APP decomposition catalyzed the formation of residual carbon, which led to higher residual carbon in the flame-retardant PU composites. As shown in Table 2 and Figure 9, the flame-retardant PU composites with nano-CB-coated APP exhibited higher initial degradation temperatures and higher residual carbon rates than PU/APP. Compared with APP/PU, CBAPP/PU exhibited a higher initial PU-decomposition temperature ($T_{-5\%}$—350.4 °C) and residual carbon content at 800 °C (60.7%). In the flame-retardant mode of the condensed phase, the final residual amount of combustion is directly related to the flame-retardant effect, and the increase in the residual amount helps to form an expanded dense carbon layer on the surface of PU, improving the flame-retardant efficiency of the material. Therefore, the CBAPP flame retardant enhanced the stability of the PU composites, owing to the catalytic carbon effect of APP, which is advantageous for enhancing the flame retardancy of PU. In addition, CB can form a condensed globular crosslinked network at high temperatures [32], leading to the formation of a bridge between the CB-crosslinked network and polyphosphoric acid. This provides a protective barrier for mass and heat transfer, thereby reducing the thermal decomposition rate of the material at high temperatures. APP and PU undergo a series of esterification and cross-linking reactions at high temperature to form a molten carbon layer, and the ammonia and water vapor generated by APP decomposition and the gas generated by PU decomposition make the molten carbon layer foam and form an expanded carbon layer on the PU surface, which prevents oxygen and PU contact with the flame, heat insulation, the production of burning droplets, and other functions. At the same time, non-combustible gases such as ammonia and water vapor can also reduce the oxygen concentration on the surface of PU, jointly playing the flame-retardant role.

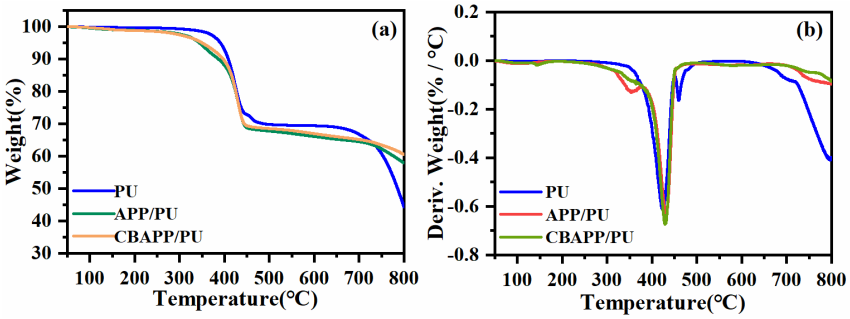


Figure 9. TGA (**a**) and DTG (**b**) curves for PU, APP/PU, and CBAPP/PU.

Table 3. TGA and DTG data for APP and CBAPP.

Samples	$T_{-5\%}$/°C	T_{max1}/°C	T_{max2}/°C	T_{max3}/°C	Residual Amount at 800 °C/wt%
APP	334.1	342.9	611.3	748.1	15.4
12% CBAPP	329.0	332.7	619.1	—	38.3

3.2.3. Flame Retardancy

To investigate the compatibility between the flame retardant and PU, the fracture surface of the PU composite was observed via SEM (Figure 10a,c). As depicted in Figure 10a, the unmodified APP displayed disordered stacking. The interface between APP and PU was distinct, and numerous APP particles exhibited poor compatibility with the PU interface, leading to weak interfacial bonding. As shown in Figure 10c, CBAPP was well dispersed in the PU matrix, displaying a smooth interface and regular stacking of fillers. The interface between the CB-modified flame retardant and the PU matrix was significantly enhanced, promoting the dispersion of CBAPP and thereby improving the mechanical properties of the PU composites.

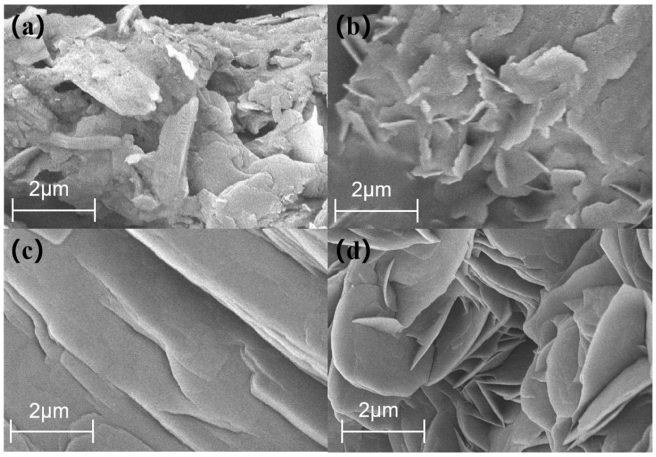


Figure 10. Pre-combustion SEM images of APP/PU (**a**) and CBAPP/PU (**c**). Post-combustion SEM images of APP/PU (**b**) and CBAPP/PU (**d**).

The SEM images of APP/PU and CBAPP/PU after combustion are shown in Figure 10b,d. The APP/PU surface exhibited a significant small-area lamellar structure (Figure 10b). In contrast, the CBAPP/PU surface formed numerous petal-like lamellar structures (Figure 10d), which effectively prevented the entry of oxygen. The modified flame retardants had two important effects on the thermal degradation and combustion of the PU matrix. First, the presence of the carbon layer enhanced the physical barrier effect of PU [33,34], preventing the diffusion of oxygen into the PU matrix and reducing the diffusion rate of volatile products to the combustion zone through penetration–vaporization. Second, the protective

layer acted as a heat shield during the combustion process. Therefore, the enhanced APP in the condensed phase improved the thermal stability and flame retardancy of PU.

The flame-retardant properties of PU and its related composites were investigated through LOI measurements and a vertical burning test (UL-94). The results are shown in Table 4. The oxygen index value of pure PU was 23.5% (Table 4), indicating flammability. In the UL-94 test, the test strip burned to the end once ignited; hence, there was no rating. With the addition of 20% (by mass) APP to PU, the LOI value of PU/APP increased to 34.4% and reached V-0 in the UL-94 test. During the burning process, the test strip quickly formed an expanding dense carbon layer to prevent the flame from spreading, and no dripping occurred. Upon the addition of CBAPP to PU, the oxygen index value of the composite was increased to 41.5% [35,36] and the LOI value was still V-0 in the UL-94 test, which indicates that the modification with CBAPP improved the flame retardancy of PU. In the UL-94 test, the combustion states of PU, APP/PU, and CBAPP/PU after ignition are shown in Supplementary Figure S2. The test results are shown below. Figure S2a: The polyurethane material is flammable, divided into two ignitions, with a total burning time of 136 s. Figure S2b,c: After adding the flame-retardant ammonium polyphosphate, neither are ignited, indicating that the addition of flame-retardant ammonium polyphosphate can increase the flame retardancy of the material. Figure S2c: The addition of CBAPP increased the oxygen index, which indicates that the addition of CBAPP did not change the flame retardancy of the materials and further increased the oxygen index, which was conducive to the improvement of the overall performance of the materials.

Table 4. Flame-retardant properties of PU, APP/PU, and CBAPP/PU.

Samples	APP/wt%	CBAPP/wt%	PU/wt%	LOI/vol%	UL-94 (Grade)
PU	0	0	100	23.5	NR
APP/PU	20	0	80	34.4	V-0
CBAPP/PU	0	20	80	41.5	V-0

3.2.4. Mechanism of Action of CBAPP/PU Composites

According to the aforementioned results, the flame-retardation mechanism of CBAPP/PU composites is proposed in Figure 11. The enhancement of PU is attributed to the following effects [37]. First, the "trapping radical" property of CB and APP derivatives enables the effective capture of peroxyl radicals and hydrogen radicals, thereby delaying or inhibiting the release of PU degradation products into the gas phase. Additionally, the chemical reaction between CB and APP during combustion forms a crosslinked network, strengthening the structure of the carbon protective layer. This "insulation effect" limits heat transfer and the diffusion of volatile thermo-oxidative products and oxygen from the gas phase to the PU. In conclusion, CB exhibits a significant flame-retardant effect when combined with APP. In the LOI, UL-94, and thermogravimetric tests, CB and APP synergistically enhanced the thermal stability and flame retardancy of PU.

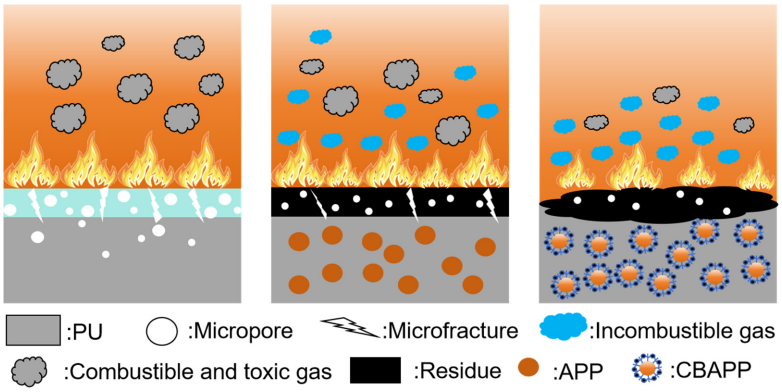


Figure 11. Schematic of the flame-retardation mechanisms of CB and APP in the PU system.

4. Conclusions

In this paper, nano carbon black microcapsule APP (CBAPP) was successfully prepared by a simple method. The results show the following: (1) The addition of APP significantly reduces the mechanical properties of PU composites, mainly due to poor compatibility. The greater the CB content in CBAPP, the higher the tensile strength of the CBAPP flame-retardant PU composite. This is due to the strong interaction between the anchored CB and PU molecular chains, which enhances the dispersion and compatibility of CBAPP in PU. (2) Compared with pure PU and APP flame-retardant PU1, PU5 containing 12% CBAPP had a higher LOI value, thermal stability, and flame retardancy. The improved thermal stability and flame retardancy can be attributed to the role of nano carbon black as a crosslinking agent, which increases the amount of carbon residue. (3) The synergistic effect of CB and APP forms a cross-linked network, forming a better carbon layer in the condensed phase, which enhances the "isolation effect". In summary, the carbon black nanoparticle-anchoring APP (CBAPP) introduced in this paper provides an effective strategy for improving the mechanical properties, flame retardancy, and thermal stability of PU composites.

Supplementary Materials: The following supporting information can be downloaded at: https://www.mdpi.com/article/10.3390/coatings14091126/s1, Figure S1. FTIR spectra of PU, APP/PU and CBAPP/PU. Figure S2. The combustion state of (a) PU, (b) APP/PU, and (c) CBAPP/PU after ignition.

Author Contributions: Research and experimental work, L.F. and W.H.; data analysis, K.Z., J.W. and Z.W.; revision, J.B. and B.X. All authors have read and agreed to the published version of the manuscript.

Funding: This study was financially supported by the Haikou Major Science and Technology Plan Project (No. 2022-006) and the Haikou Major Science and Technology Plan Project (No. 2021-010).

Institutional Review Board Statement: Not applicable.

Informed Consent Statement: Not applicable.

Data Availability Statement: Data are contained within the article.

Conflicts of Interest: Author Zhong Wang was employed by Hainan Sequoia Technology Co., Ltd. The remaining authors declare that the research was conducted in the absence of any commercial or financial relationships that could be construed as a potential conflict of interest.

References

1. Somarathna, H.M.C.C.; Raman, S.N.; Mohotti, D.; Mutalib, A.A.; Badri, K.H. The use of polyurethane for structural and infrastructural engineering applications: A state-of-the-art review. *Constr. Build. Mater.* **2018**, *190*, 995–1014. [CrossRef]
2. Wan, L.; Deng, C.; Chen, H.; Zhao, Z.-Y.; Huang, S.-C.; Wei, W.-C.; Yang, A.-H.; Zhao, H.-B.; Wang, Y.-Z. Flame-retarded thermoplastic polyurethane elastomer: From organic materials to nanocomposites and new prospects. *Chem. Eng. J.* **2021**, *417*, 129314. [CrossRef]
3. Jia, P.; Zhu, Y.; Lu, J.; Wang, B.; Song, L.; Wang, B.; Hu, Y. Multifunctional fireproof electromagnetic shielding polyurethane films with thermal management performance. *Chem. Eng. J.* **2022**, *439*, 135673. [CrossRef]
4. Sun, Z.; Wen, J.; Wang, W.; Fan, H.; Chen, Y.; Yan, J.; Xiang, J. Polyurethane covalently modified polydimethylsiloxane (PDMS) coating with increased surface energy and re-coatability. *Prog. Org. Coat.* **2020**, *146*, 105744. [CrossRef]
5. Castellano, A.; Colleoni, C.; Iacono, G.; Mezzi, A.; Plutino, M.R.; Malucelli, G.; Rosace, G. Synthesis and characterization of a phosphorous/nitrogen based sol-gel coating as a novel halogen- and formaldehyde-free flame retardant finishing for cotton fabric. *Polym. Degrad. Stab.* **2019**, *162*, 148. [CrossRef]
6. Zhang, P.; Xu, P.; Fan, H.; Sun, Z.; Wen, J. Covalently functionalized graphene towards molecular-level dispersed waterborne polyurethane nanocomposite with balanced comprehensive performance. *Appl. Surf. Sci.* **2019**, *471*, 595–606. [CrossRef]
7. Zhou, Y.; Bu, R.; Gong, J.; Yan, W.; Fan, C. Experimental investigation on downward flame spread over rigid polyurethane and extruded polystyrene foams. *Exp. Therm. Fluid Sci.* **2018**, *92*, 346–352. [CrossRef]
8. Song, S.; Ma, J.; Cao, K.; Chang, G.; Huang, Y.; Yang, J. Synthesis of a novel dicyclic silicon-/phosphorus hybrid and its performance on flame retardancy of epoxy resin. *Polym. Degrad. Stab.* **2014**, *99*, 43–52. [CrossRef]
9. Cao, Y.; Zhou, M.; Wang, S.; Fu, H. Superhydrophobic and flame retardant polydimethylsiloxane coatings with layered double hydroxide and ammonium polyphosphate. *Prog. Org. Coat.* **2022**, *172*, 107117. [CrossRef]

10. Li, M.-E.; Wang, S.-X.; Han, L.-X.; Yuan, W.-J.; Cheng, J.-B.; Zhang, A.-N.; Zhao, H.-B.; Wang, Y.-Z. Hierarchically porous SiO_2/polyurethane foam composites towards excellent thermal insulating, flame-retardant and smoke-suppressant performances. *J. Hazard. Mater.* **2019**, *375*, 61–69. [CrossRef]
11. Guo, E.; Tang, B.; Wang, S.; Feng, W.; Wang, X.; Sun, J.; Zhang, S.; Gu, X.; Li, H. A cocktail strategy for enhancing flame retardance and water resistance of butyl acrylate coatings. *Mater. Chem. Phys.* **2021**, *263*, 124367. [CrossRef]
12. Leistner, M.; Haile, M.; Rohmer, S.; Abu-Odeh, A.; Grunlan, J.C. Water-soluble polyelectrolyte complex nanocoating for flame retardant nylon-cotton fabric. *Polym. Degrad. Stab.* **2015**, *122*, 1–7. [CrossRef]
13. Sun, Y.; Yuan, B.; Shang, S.; Zhang, H.; Shi, Y.; Yu, B.; Qi, C.; Dong, H.; Chen, X.; Yang, X. Surface modification of ammonium polyphosphate by supramolecular assembly for enhancing fire safety properties of polypropylene. *Compos. Part B Eng.* **2020**, *181*, 107588. [CrossRef]
14. Eceiza, I.; Aguirresarobe, R.; Barrio, A.; Fernández-Berridi, M.J.; Irusta, L. Ammonium polyphosphate-melamine synergies in thermal degradation and smoke toxicity of flexible polyurethane foams. *Thermochim. Acta* **2023**, *726*, 179554. [CrossRef]
15. Zhao, Z.; Jin, Q.; Zhang, N.; Guo, X.; Yan, H. Preparation of a novel polysiloxane and its synergistic effect with ammonium polyphosphate on the flame retardancy of polypropylene. *Polym. Degrad. Stab.* **2018**, *150*, 73–85. [CrossRef]
16. Tang, Y.; Tang, C.; Hu, D.; Gui, Y. Effect of Aminosilane Coupling Agents with Different Chain Lengths on Thermo-Mechanical Properties of Cross-Linked Epoxy Resin. *Nanomaterials* **2018**, *811*, 951. [CrossRef]
17. Meng, L.; Li, X.; Liu, M.; Li, C.; Meng, L.; Hou, S. Modified Ammonium Polyphosphate and Its Application in Polypropylene Resins. *Coatings* **2022**, *12*, 1738. [CrossRef]
18. Hussain, A.; Landry, V.; Blanchet, P.; Hoang, D.; Dagenais, C. Fire Performance of Intumescent Waterborne Coatings with Encapsulated APP for Wood Constructions. *Coatings* **2021**, *11*, 1272. [CrossRef]
19. Chen, X.; Jiang, Y.; Jiao, C. Smoke suppression properties of ferrite yellow on flame retardant thermoplastic polyurethane based on ammonium polyphosphate. *J. Hazard. Mater.* **2014**, *266*, 114–121. [CrossRef]
20. Dasari, A.; Yu, Z.-Z.; Cai, G.-P.; Mai, Y.-W. Recent developments in the fire retardancy of polymeric materials. *Prog. Polym. Sci.* **2013**, *389*, 1357–1387. [CrossRef]
21. Shi, X.; Pan, Y.; Wang, Y.; Jia, Z.; Chen, T.; Gong, J.; Jiang, J. Synergistic Effects of Graphene and Ammonium Polyphosphate Modified with Vinyltrimethoxysilane on the Properties of High-Impact Polystyrene Composites. *Polymers* **2021**, *136*, 881. [CrossRef]
22. Ren, Y.; Yuan, D.; Li, W.; Cai, X. Flame retardant efficiency of KH-550 modified urea-formaldehyde resin cooperating with ammonium polyphosphate on polypropylene. *Polym. Degrad. Stab.* **2018**, *151*, 160–171. [CrossRef]
23. Wang, B.; Jia, P.; Zhang, Y.; He, R.; Song, L.; Hu, Y. Multifunctional composite polyvinyl alcohol films prepared with economic conductive carbon black and MXene microcapsuled APP. *Mater. Today Phys.* **2023**, *30*, 100928. [CrossRef]
24. Liu, C.; Yao, A.; Chen, K.; Shi, Y.; Feng, Y.; Zhang, P.; Yang, F.; Liu, M.; Chen, Z. MXene based core-shell flame retardant towards reducing fire hazards of thermoplastic polyurethane. *Compos. Part B Eng.* **2021**, *226*, 109363. [CrossRef]
25. Yang, H.; Guan, Y.; Ye, L.; Wang, S.; Li, S.; Wen, X.; Chen, X.; Mijowska, E.; Tang, T. Synergistic effect of nanoscale carbon black and ammonium polyphosphate on improving thermal stability and flame retardancy of polypropylene: A reactive network for strengthening carbon layer. *Compos. Part B Eng.* **2019**, *174*, 107038. [CrossRef]
26. Yu, R.; Liu, J.; Gao, D.; Wang, Y.; Wen, X.; Tang, T. Striking effect of nanosized carbon black modified by grafting sodium sulfonate on improving the flame retardancy of polycarbonate. *Compos. Commun.* **2020**, *20*, 100359. [CrossRef]
27. Wang, Y.; Zhao, J. Benign design of intumescent flame retardant coating incorporated various carbon sources. *Constr. Build. Mater.* **2020**, *236*, 117433. [CrossRef]
28. Shao, Z.-B.; Cui, J.; Li, X.-L.; Díaz Palencia, J.L.; Wang, D.-Y. Chemically inorganic modified ammonium polyphosphate as eco-friendly flame retardant and its high fire safety for epoxy resin. *Compos. Commun.* **2021**, *28*, 100959. [CrossRef]
29. Zielecka, M.; Rabajczyk, A.; Pastuszka, Ł.; Jurecki, L. Flame Resistant Silicone-Containing Coating Materials. *Coatings* **2020**, *105*, 479. [CrossRef]
30. Jiang, B.; Ding, D.; Su, M.; Lu, K.; Yu, C.; Ji, B.; Hong, H. Experimental study on the explosion suppression characteristics of polyethylene dust by ammonium polyphosphate. *Powder Technol.* **2024**, *437*, 119491. [CrossRef]
31. Wan, M.; Shi, C.; Qian, X.; Qin, Y.; Jing, J.; Che, H.; Ren, F.; Li, J.; Yu, B.; Zhou, K. Design of novel double-layer coated ammonium polyphosphate and its application in flame retardant thermoplastic polyurethanes. *Chem. Eng. J.* **2023**, *459*, 141448. [CrossRef]
32. Wen, X.; Wang, Y.; Gong, J.; Liu, J.; Tian, N.; Wang, Y.; Jiang, Z.; Qiu, J.; Tang, T. Thermal and flammability properties of polypropylene/carbon black nanocomposites. *Polym. Degrad. Stab.* **2012**, *975*, 793–801. [CrossRef]
33. Cao, X.; Zhao, W.; Huang, J.; He, Y.; Liang, X.; Su, Y.; Wu, W.; Li, R.K.Y. Interface engineering of graphene oxide containing phosphorus/nitrogen towards fire safety enhancement for thermoplastic polyurethane. *Compos. Commun.* **2021**, *27*, 100821. [CrossRef]
34. Gao, D.; Wen, X.; Guan, Y.; Czerwonko, W.; Li, Y.; Gao, Y.; Mijowska, E.; Tang, T. Flame retardant effect and mechanism of nanosized NiO as synergist in PLA/APP/CSi-MCA composites. *Compos. Commun.* **2020**, *17*, 170–176. [CrossRef]
35. Yan, J.; Xu, P.; Zhang, P.; Fan, H. Surface-modified ammonium polyphosphate for flame-retardant and reinforced polyurethane composites. *Colloids Surf. A Physicochem. Eng. Asp.* **2021**, *626*, 127092. [CrossRef]

36. Cui, M.; Li, J.; Chen, X.; Hong, W.; Chen, Y.; Xiang, J.; Yan, J.; Fan, H. A halogen-free, flame retardant, waterborne polyurethane coating based on the synergistic effect of phosphorus and silicon. *Prog. Org. Coat.* **2021**, *158*, 106359. [CrossRef]
37. Piao, J.; Lai, Y.; Ren, J.; Wang, Y.; Feng, T.; Wang, Y.; Liu, W.; Dong, H.; Chen, W.; Jiao, C.; et al. Zn-doped carbon microspheres as synergist in intumescent flame-retardant thermoplastic polyurethane composites: Mechanism of char residues layer regulation. *Compos. Commun.* **2022**, *32*, 101173. [CrossRef]

Disclaimer/Publisher's Note: The statements, opinions and data contained in all publications are solely those of the individual author(s) and contributor(s) and not of MDPI and/or the editor(s). MDPI and/or the editor(s) disclaim responsibility for any injury to people or property resulting from any ideas, methods, instructions or products referred to in the content.